Supporting Information

Mole-Ratio Dependent Reversible Transformation between 2:2 and Cyclic 3:6 Silver(I) Complexes with an Argentivorous Molecule

Huiyeong Ju,[†] Tomoko Abe,[†] Yukari Takahashi,[†] Yumiko Tsuruoka,[†], Akihiro Otsuka,[†] Eunji Lee,[†,§] Mari Ikeda,[‖] Shunsuke Kuwahara[†,‡] and Yoichi Habata[*,†,‡]

[†]Department of Chemistry and [‡]Research Center for Materials with Integrated Properties, Faculty of Science, Toho University, 2-2-1Miyama, Funabashi, Chiba 274-8510, Japan
[§]Department of Chemistry, Gangneung-Wonju National University, Gangneung 25457, South Korea
[‖]Education Center, Faculty of Engineering, Chiba Institute of Technology, 2-1-1 Shibazono, Narashino, Chiba 275-0023, Japan

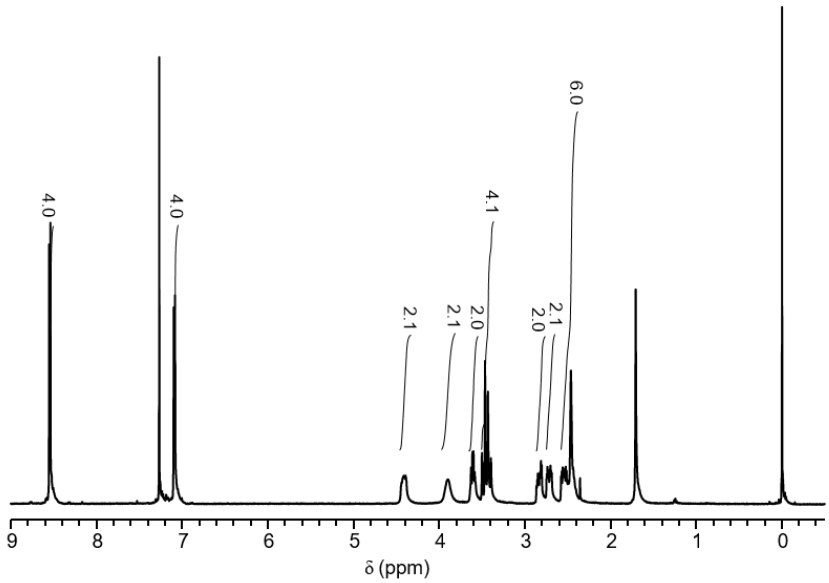

(a)

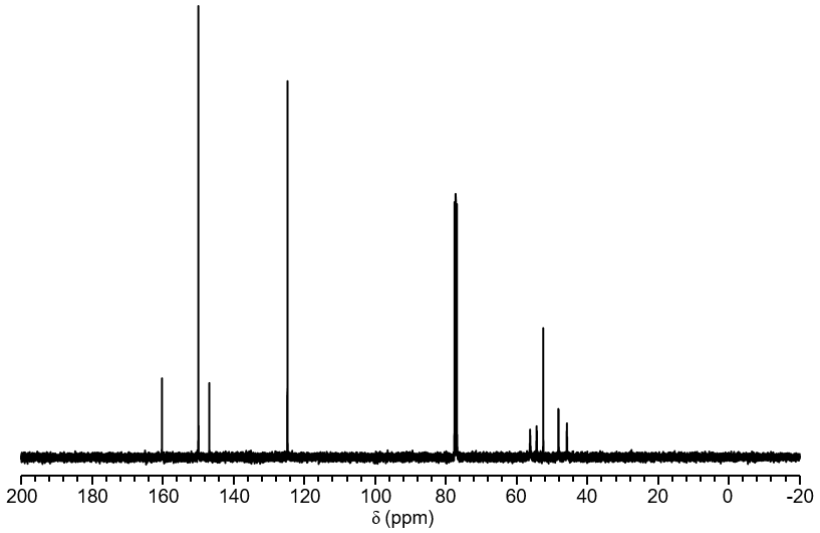

(b)

Figure S1. (a) ^{1}H and (b) ^{13}C NMR spectra of **4** in $CDCl_3$.

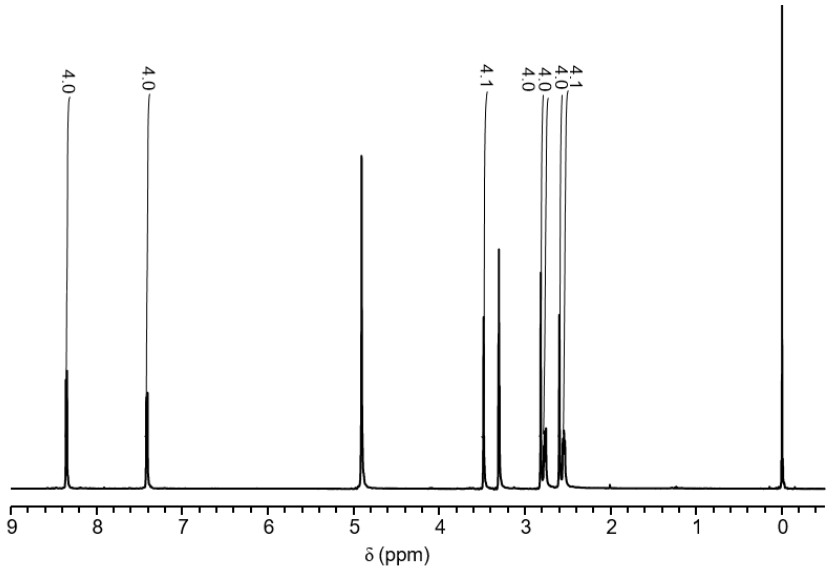

(a)

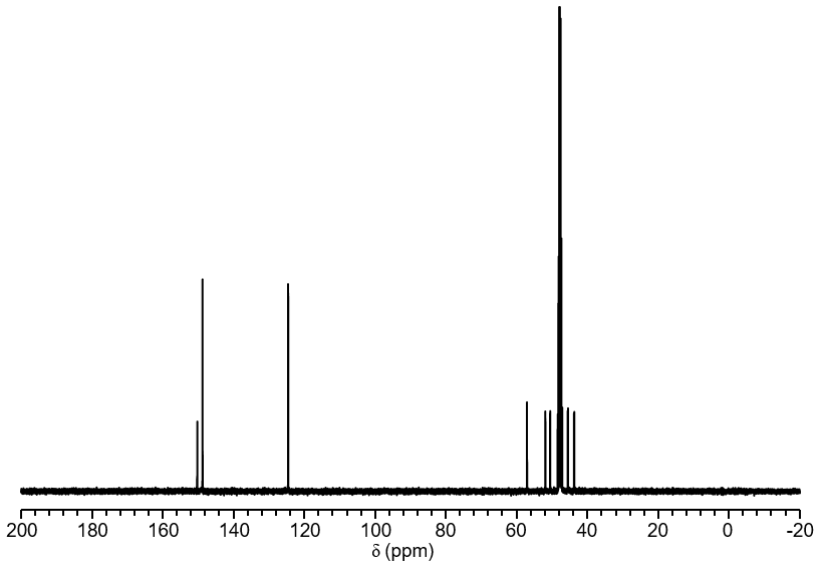

(b)

Figure S2. (a) ^{1}H and (b) ^{13}C NMR spectra of **5** in CD_3OD.

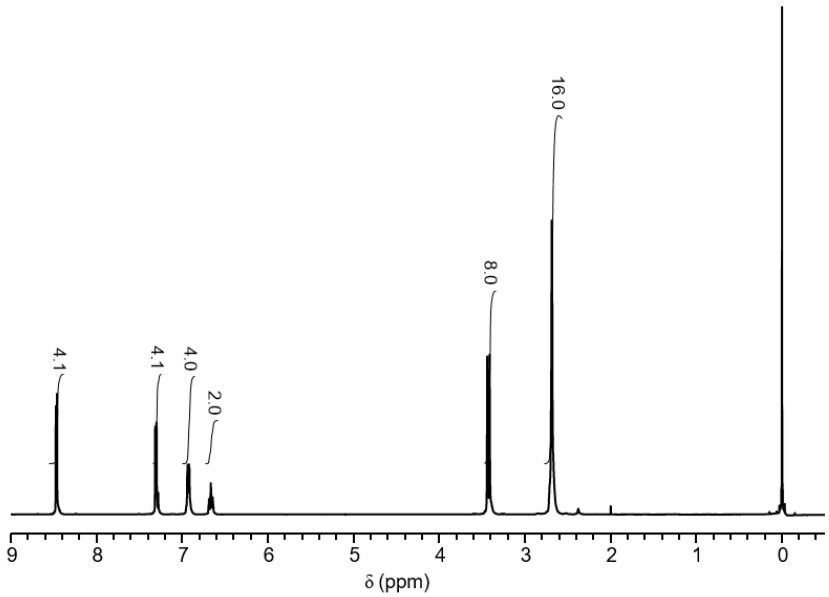

(a)

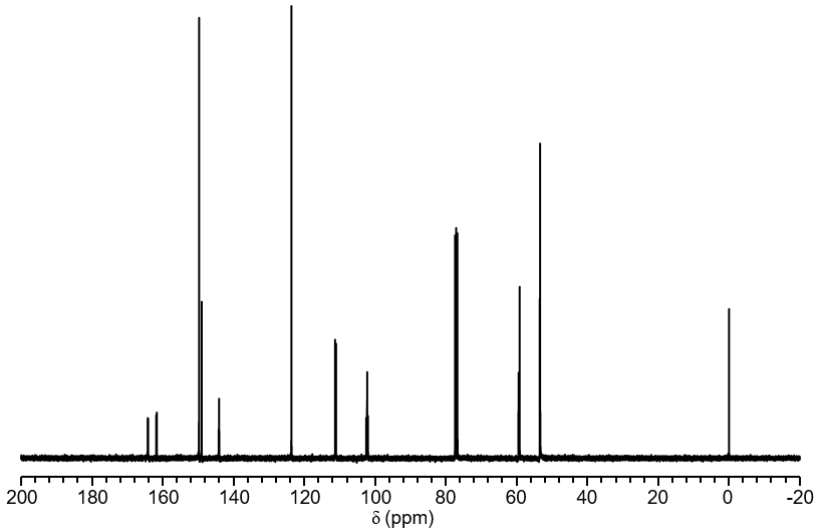

(b)

Figure S3. (a) ^{1}H and (b) ^{13}C NMR spectra of **L** in $CDCl_3$.

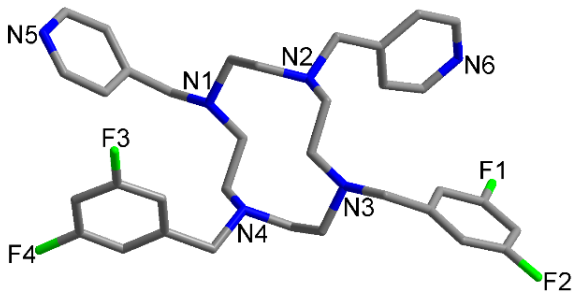

Figure S4. Crystal structure of **L**. Hydrogen atoms are omitted.

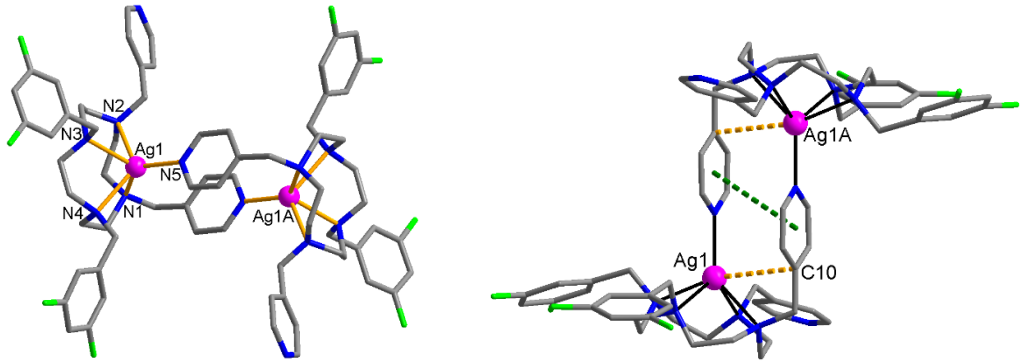

(a) (b)

Figure S5. X-ray structure of $[(\mathbf{L})_2Ag_2]^{2+}$: (a) side view and (b) Ag^+-π interaction (orange dotted line, Ag1-C10 3.281 Å) and π-π stacking (green dotted line, centroid···centroid 3.789 Å). Hydrogen atoms are omitted.

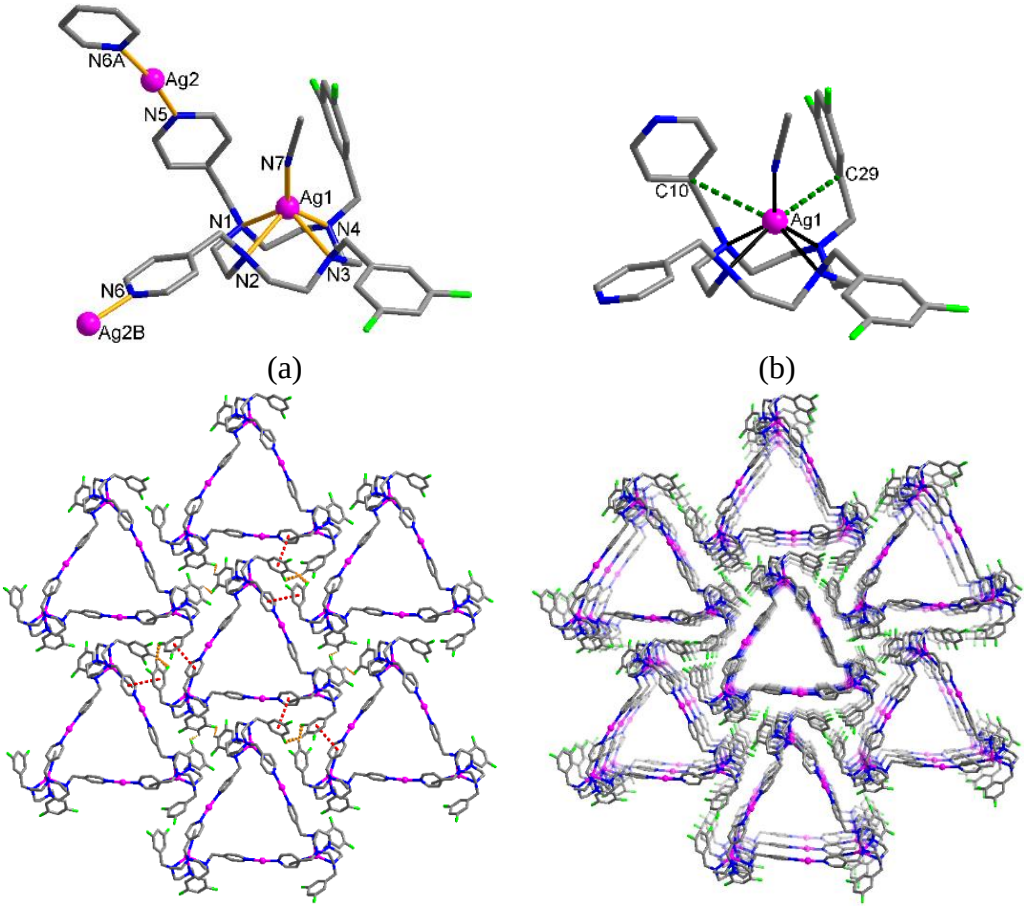

(a) (b)

(c) (d)

Figure S6. X-ray structure of $[(\mathbf{L})_3Ag_6]^{6+}$: (a) core coordination unit, (b) Ag^+-π interactions (green dotted line, Ag1-C10 3.593 and Ag1-C29 3.409 Å), (c) packing structure showing the *pseudo*-2D layer via intermolecular interactions including π-π stacking (red dotted line, 4.037 Å) and C-H···F interactions (orange dotted line, 2.664 and 2.829 Å), and (d) channel structure formed by stacking of *pseudo*-2D layers. Hydrogen atoms are omitted.

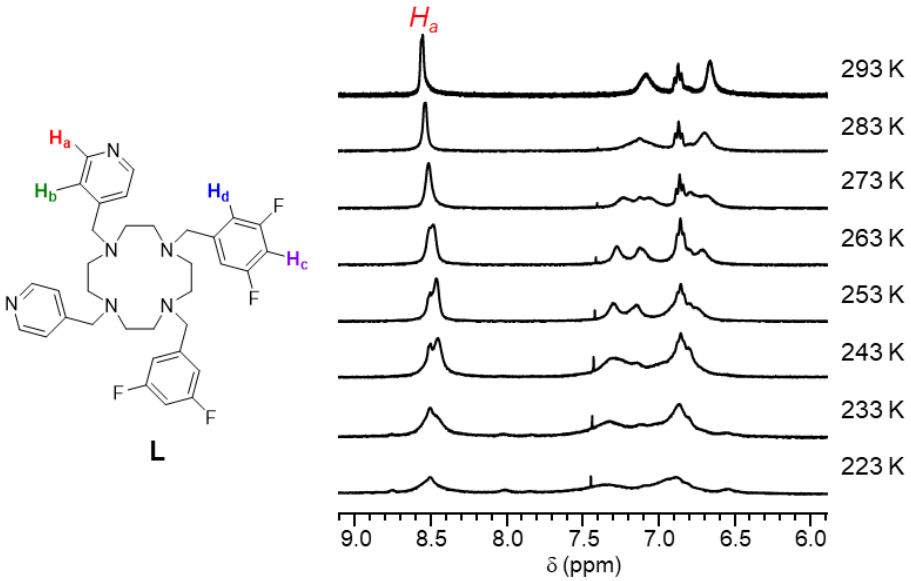

Figure S7. VT-NMR (223-293 K) spectra of the aromatic region for **L** (4 mM in CD_2Cl_2) with 1.0 equiv of silver(I) (0.5 M in CD_3OD). [**L**] = 0.80 x 10^{-3} M.

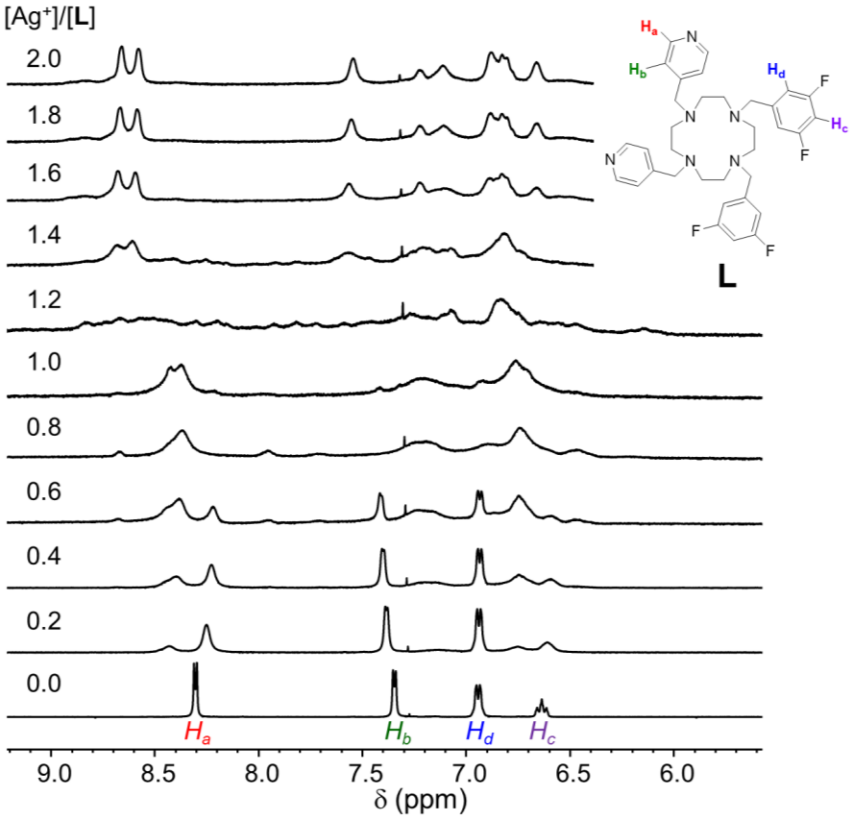

Figure S8. Ag^+-induced ^1H NMR spectral changes of **L** in a mixture of CD_2Cl_2/CD_3OD at 243K. [**L**] = 0.80 x 10^{-3} M.

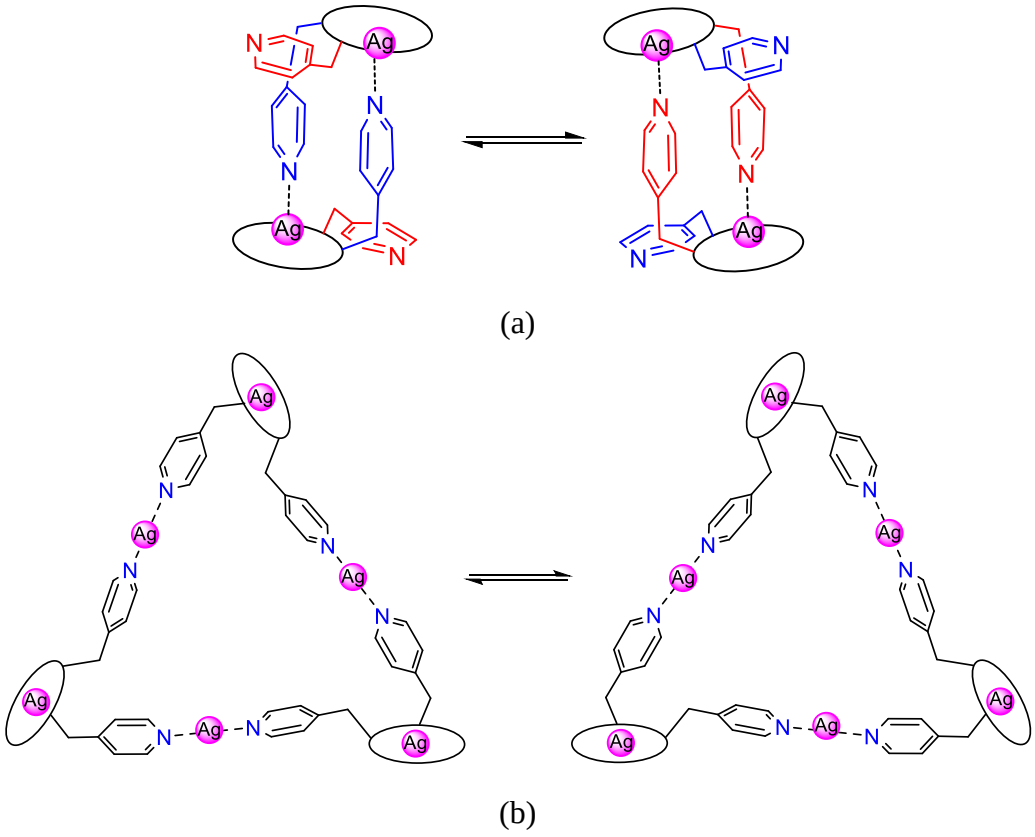

Figure S9. Postulated conformational changes of (a) the 2:2 and (b) 3:6 (= **L**:Ag^+) complexes.

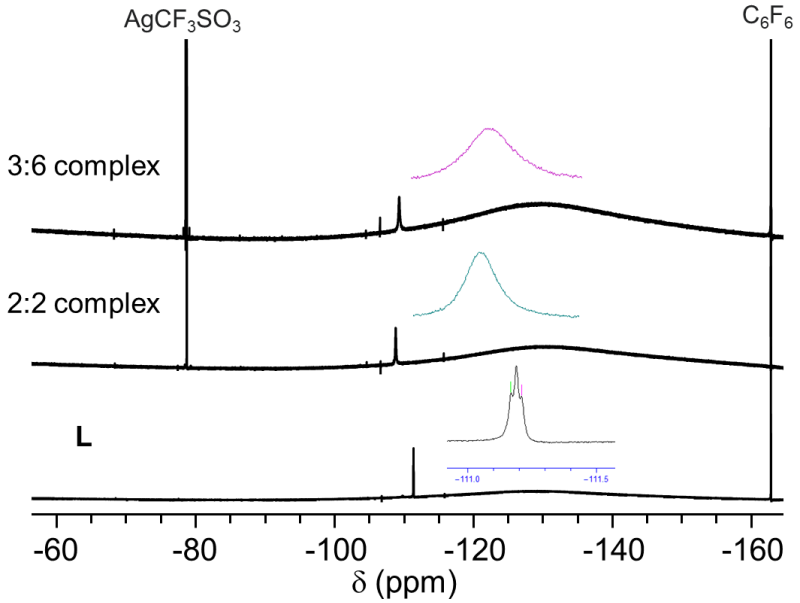

Figure S10. $^{19}F\{^1H\}$ NMR spectra (376 MHz, 298 K, CD_2Cl_2) of **L**, 2:2 (**L**:Ag^+) complex, and 3:6 (**L**:Ag^+) complex. Expanded signals were inserted. The inserted signals are the enlarged signals of ^{19}F signals in the 3,5-difluorobenzyl groups.

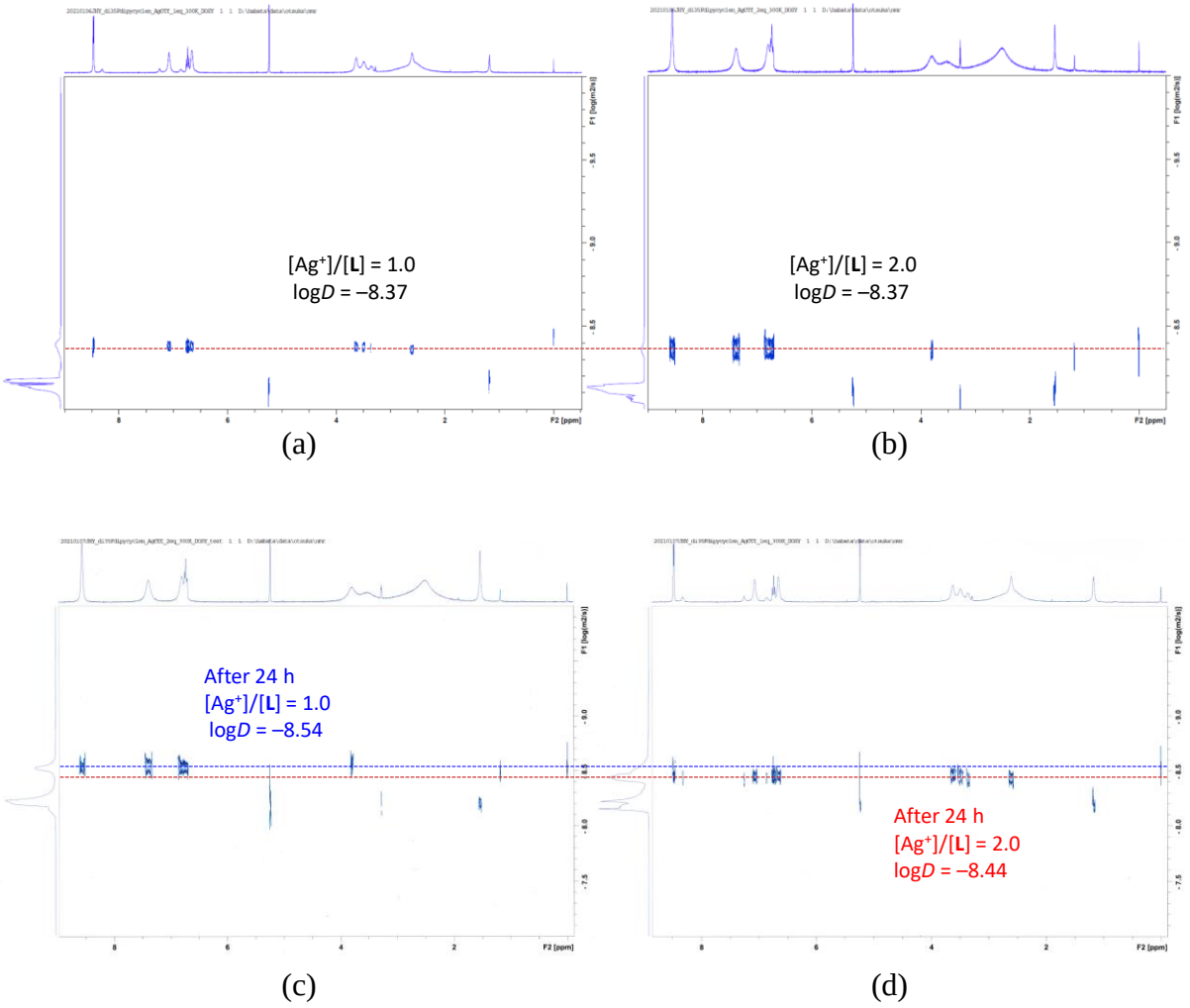

Figure S11. Diffusion-ordered spectroscopy (DOSY) NMR spectra of **L** and AgOTf in CD_2Cl_2/CD_3OD at 300 *K*, [**L**] = 8.0 x 10^{-3} M. Figures S10 (a) and (b) were measured immediately after the mixing of **L** and Ag^+, and (c) and (d) were measured after 24 hours. (a) $[Ag^+]/[\mathbf{L}]$ = 1.0 and (b) $[Ag^+]/[\mathbf{L}]$ = 2.0. The experimental diffusion coefficients of the 1:1 and 1:2 (= **L** : Ag^+) mixtures were 4.27 × 10^{-9} m^2/s. (c) $[Ag^+]/[\mathbf{L}]$ = 1.0 and (d) $[Ag^+]/[\mathbf{L}]$ = 2.0. The experimental diffusion coefficients of the 1:1 and 1:2 (= **L** : Ag^+) mixtures were 3.63 × 10^{-9} and 2.88 × 10^{-9} m^2/s, respectively.

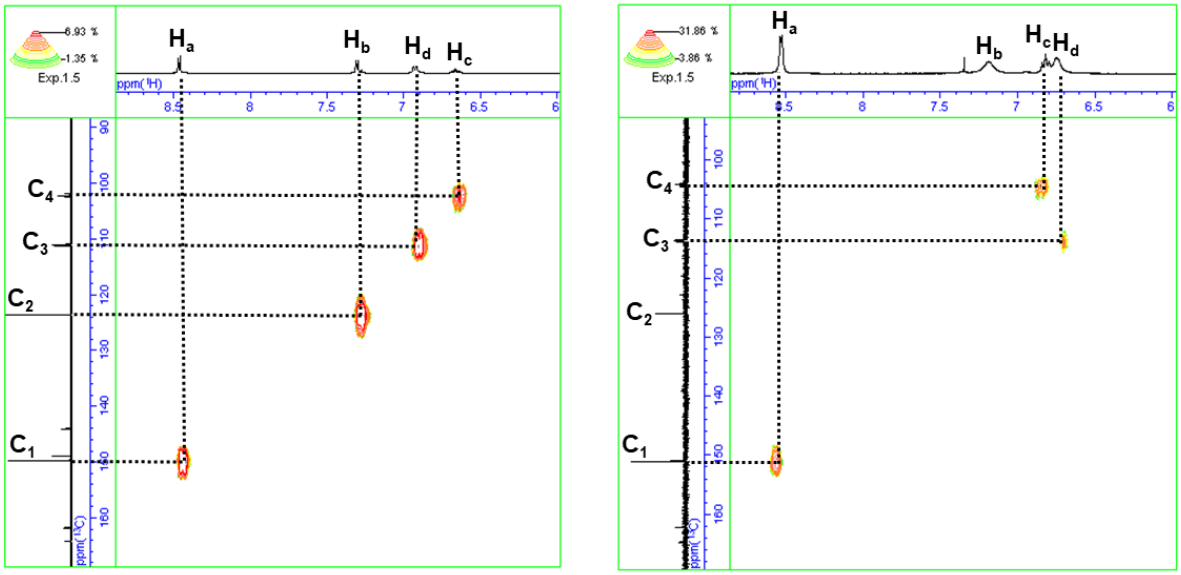

(a) (b)

Figure S12. 2D HMQC NMR spectra of the aromatic part: (a) [Ag^+]/[**L**] = 0.0 and (b) [Ag^+]/[**L**] = 1.0.

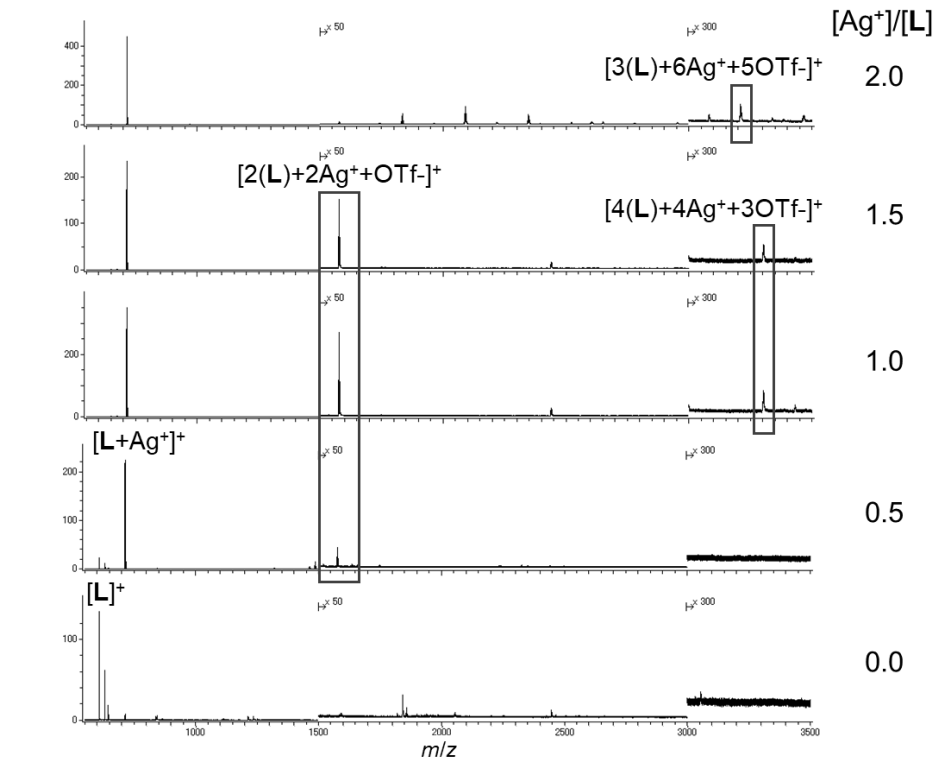

(a)

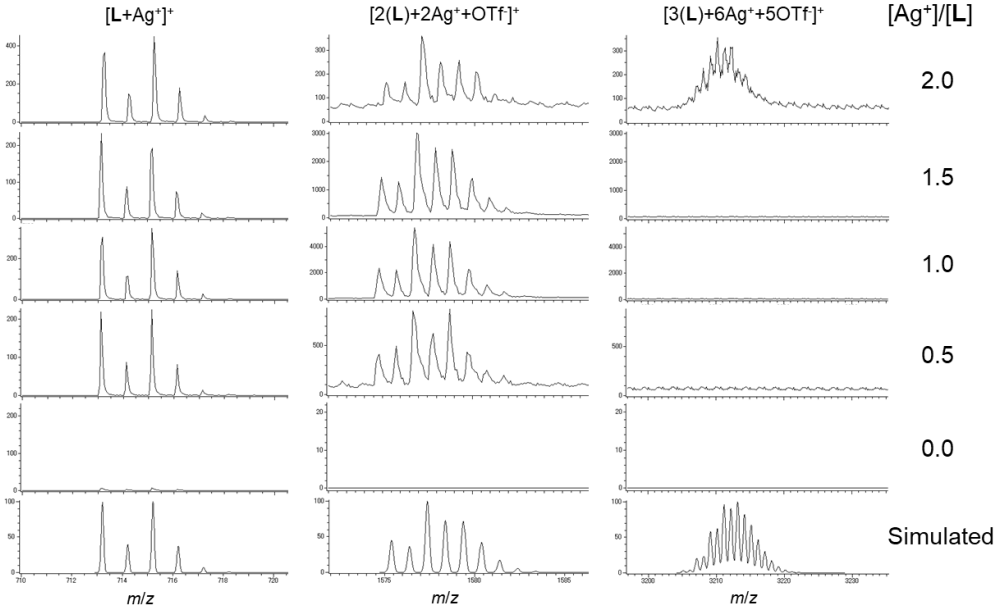

(b)

Figure S13. (a) CSI-mass spectra of **L** (5.0×10^{-4} M) in the presence of different mole ratios of AgOTf in CH_3OH and (b) observed ion peaks (top) and theoretical distributions (bottom).

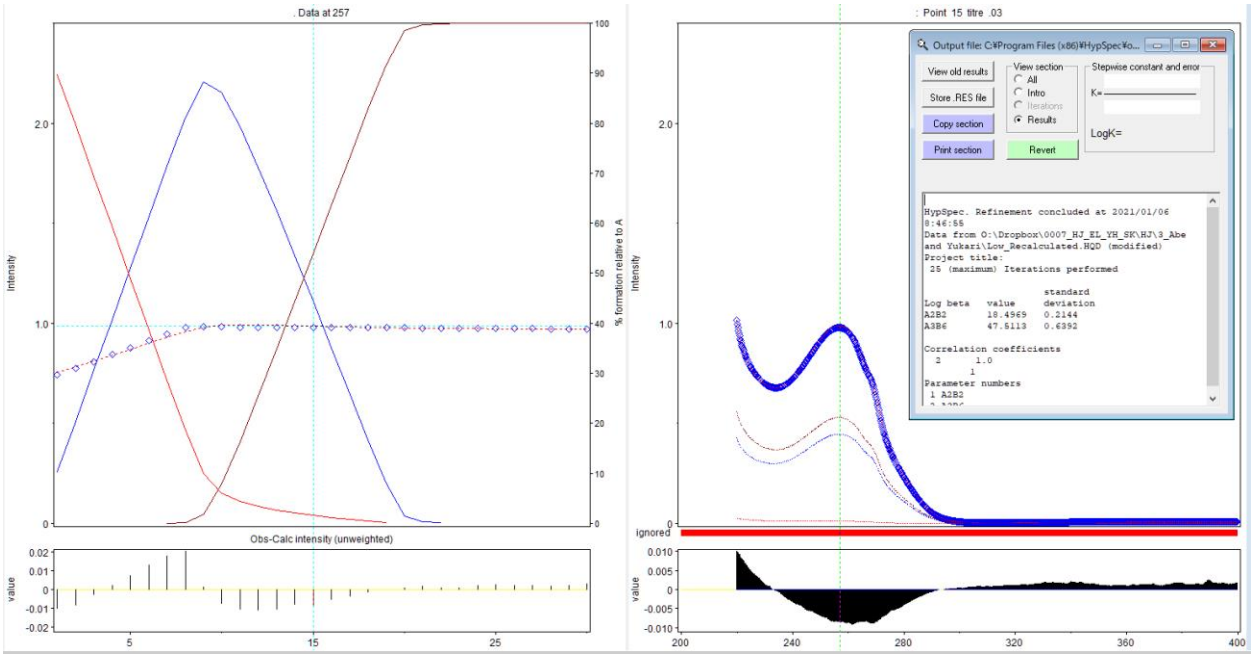

(a)

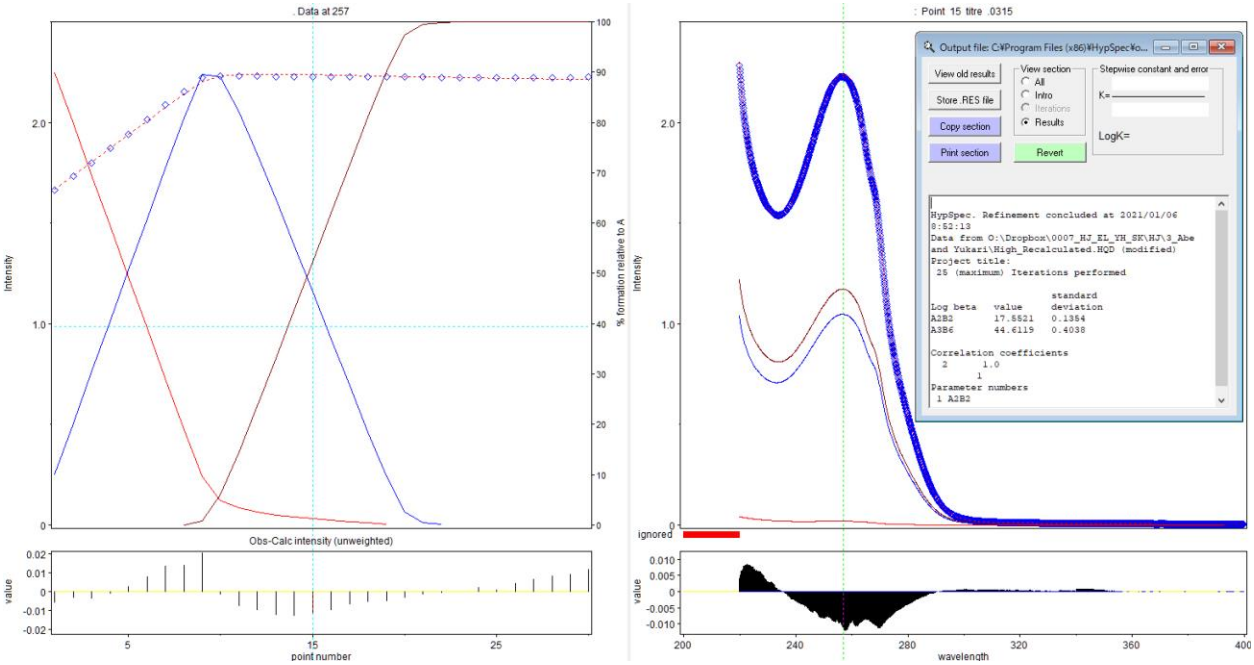

(b)

Figure S14. HyperSpec^{TM} output for UV-Vis spectral titration of **L** upon addition of silver(I) triflate in acetonitrile: (a) [**L**] = 1.5 × 10^{-4} M and (b) [**L**] = 3.4 × 10^{-4} M. Blue and brown curves in the titration plots at 257 nm are the % formation of $\mathbf{L}_2Ag_2$ and $\mathbf{L}_3Ag_6$ relative to **L**, respectively.

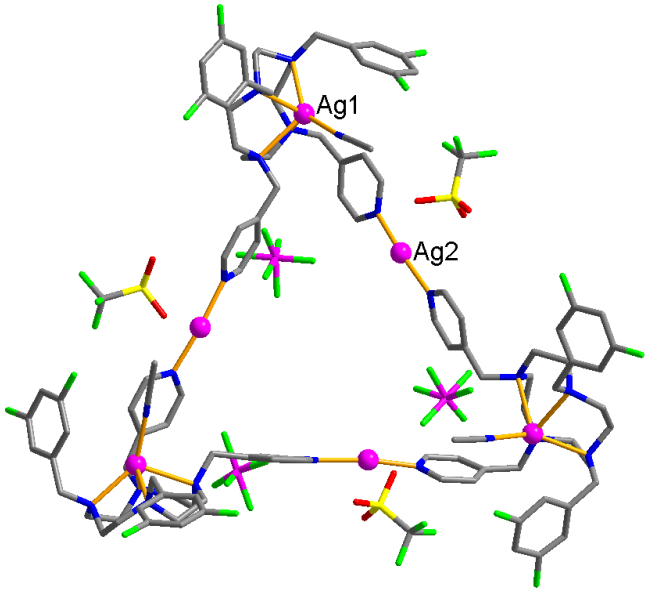

Figure S15. X-ray structure of a 3:6 cyclic trimer, $[Ag_6(\mathbf{L})_3(CH_3CN)_3](OTf)_3(PF_6)_3$, which was obtained from the reaction of the 2:2 complex solution with AgOTf.

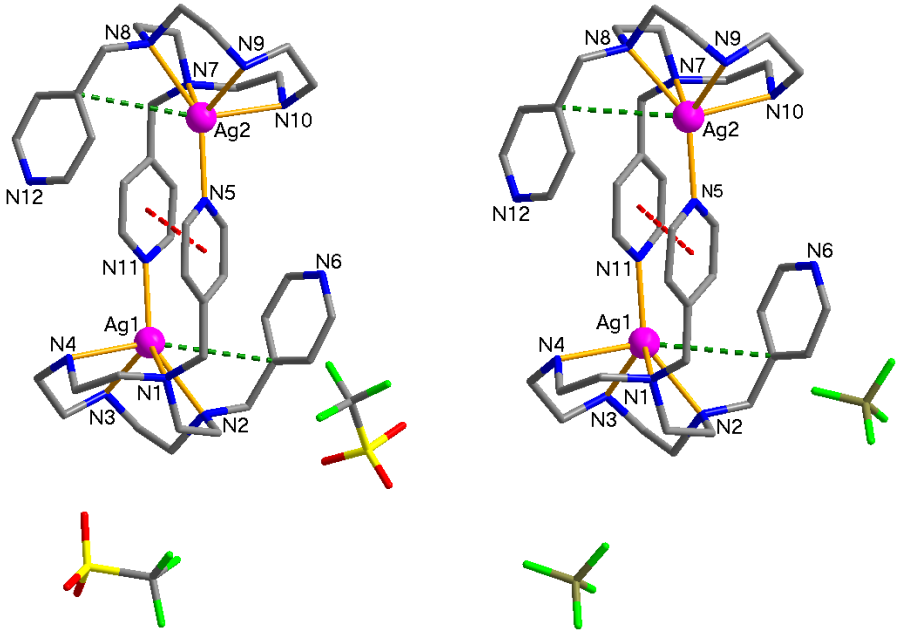

(a) (b)

Figure S16. X-ray structures of 2:2 dimer complexes of **5**: (a) $[Ag_2(\mathbf{5})_2](OTf)_2$ and (b) $[Ag_2(\mathbf{5})_2](BF_4)_2$. The Ag(I) centers of both structures are five-coordinated to an N_4-donor from the cyclen and one nitrogen atom from neighbor pyridine of **5**. Two side arms were covered the Ag^+ ion with Ag^+-π interaction (green dotted line). The π-π stacking between neighboring two pyridine units (red dotted line) is confirmed. The X-ray structures indicate that the anions have no effect on the structure of the 2:2 complexes.

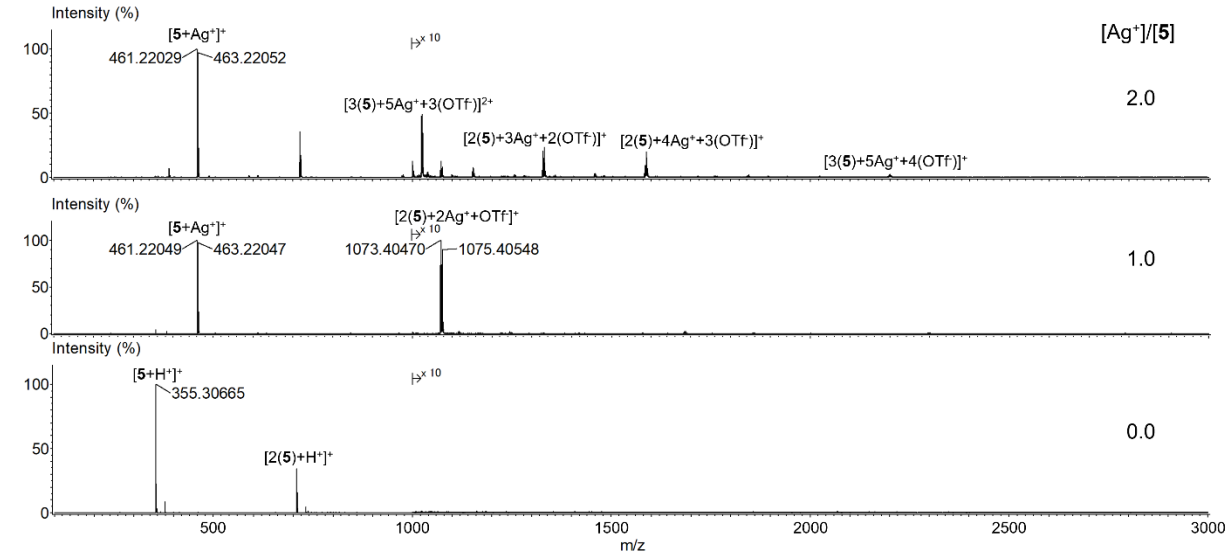

(a)

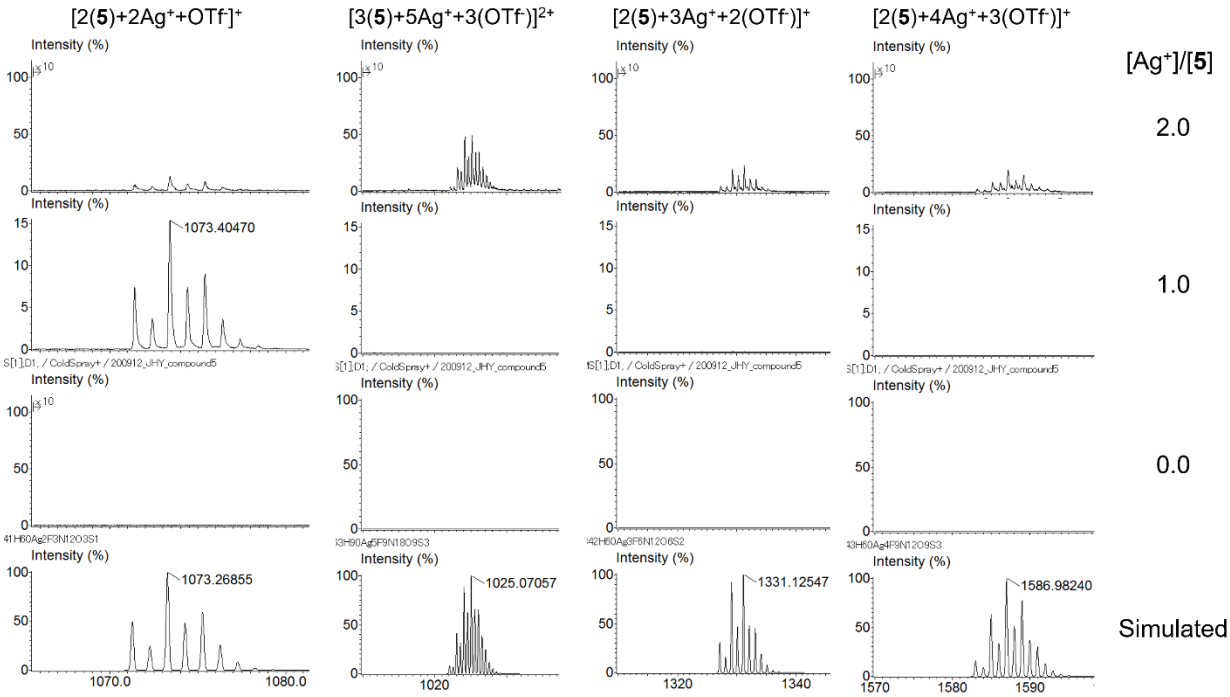

(b)

Figure S17. (a) CSI-MS spectra of **5** depending on the mole ratio of AgOTf in CH_3OH and (b) observed ion peaks (top) and theoretical distributions (bottom).

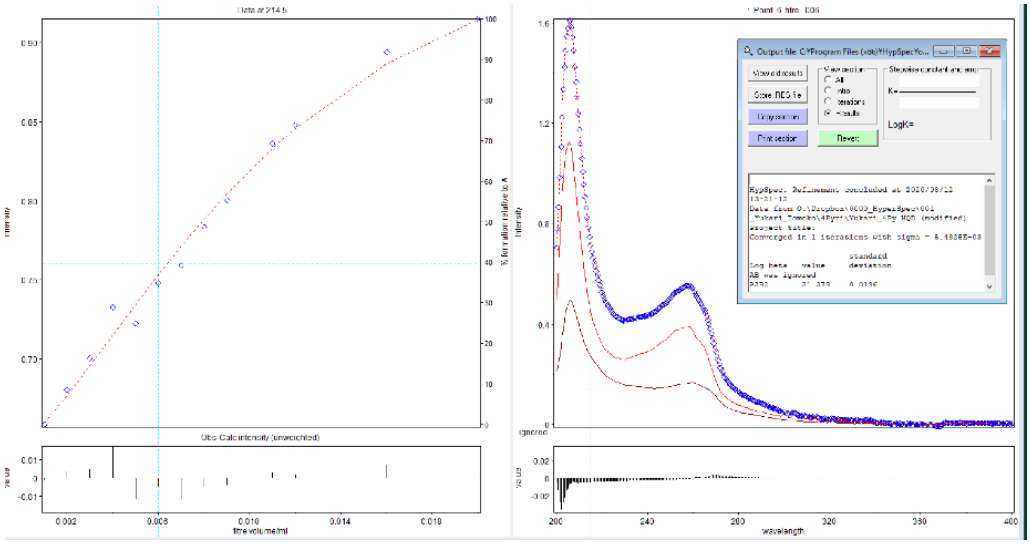

Figure S18. HyperSpec output for UV-Vis spectral changes of **5** (5.0×10^{-4} M) upon addition of silver(I) triflate in acetonitrile. The log*K* value for a 2:2 complex between **5** and Ag^{+} was determined and was estimated to be *ca.* 21.4(1).

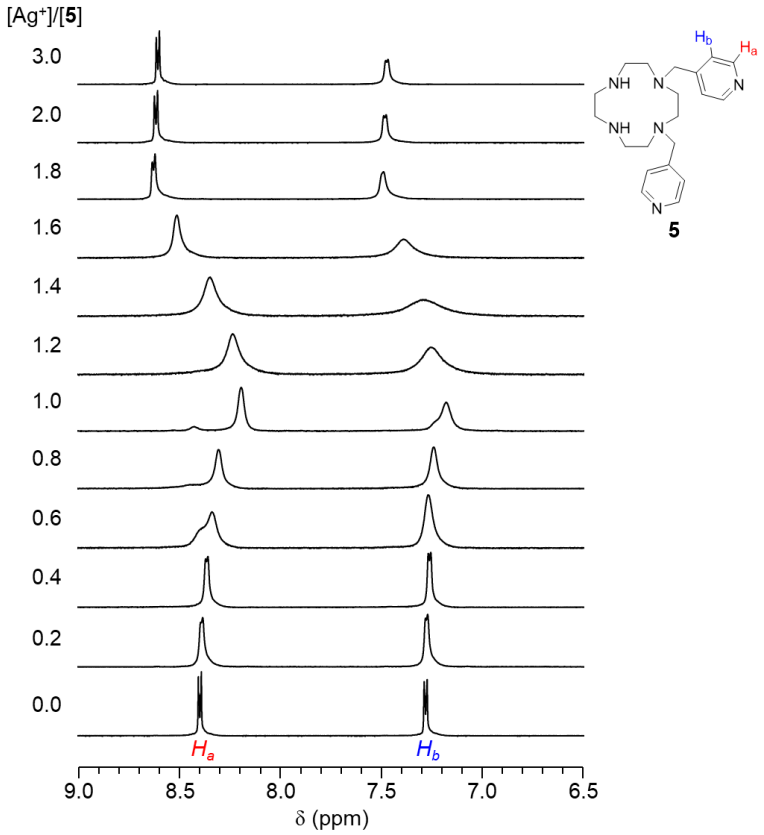

Figure S19. ^{1}H NMR spectral changes of **5** (5.0×10^{-3} M) upon addition of silver(I) triflate in CD_2Cl_2/CD_3OD.

X-ray Crystallographic Analysis

All data were collected on a Bruker SMART APEX II ULTRA diffractometer equipped with graphite monochromated Mo K_α radiation ($\lambda = 0.71073$ Å) generated by a rotating anode. The cell parameters for the compounds were obtained from a least-squares refinement of the spot. Data collection, data reduction and semi-empirical absorption correction were carried out using the software package of APEX2.[S1] All of the calculations for the structure determination were carried out using the SHELXTL package.[S2] In all cases, nonhydrogen atoms were refined anisotropically and hydrogen atoms were placed in idealized positions and refined isotropically in a riding manner along with their respective parent atoms. For the refinement of disordered atoms in $[(\mathbf{L})_2Ag_2]^{2+}$, the commands (ISOR and DFIX) have been used. Since the lattice solvent molecules in $[(\mathbf{L})_3Ag_6]^{6+}$ and $[Ag_6(\mathbf{L})_3](OTf)_3(PF_6)_3$ are highly disordered, the contribution of solvent electron density was removed by the SQUEEZE routine in PLATON.[S3] The low quality of the crystals of $[Ag_2(\mathbf{5})_2](OTf)_2$ precluded the possibility to reach data completeness >82%, however not jeopardizing the structure solution and refinement. The submitted manuscript mainly reports Ag(I) complexes of tetra-armed cyclen. While this structure is silver(I) complex of precursor compound, and it was sufficient to show the coordination environment. Relevant crystal data collection and refinement data for the crystal structures are summarized in Table S1. CCDC 2009246 (**L**), 2009247 ($[(\mathbf{L})_2Ag_2]^{2+}$), 2009248 ($[(\mathbf{L})_3Ag_6]^{6+}$), 2009249 ($[Ag_2(\mathbf{5})_2](OTf)_2$), 2009250 ($[Ag_2(\mathbf{5})_2](BF_4)_2$), and 2038878 ($[Ag_6(\mathbf{L})_3](OTf)_3(PF_6)_3$) contain the supplementary crystallographic data for this paper. These data can be obtained free of charge from The Cambridge Crystallographic Data Centre via www.ccdc.cam.ac.uk/data_request/cif.

Table S1. Crystal and Experimental Data

	L	$[(\mathbf{L})_2Ag_2]^{2+}$	$[(\mathbf{L})_3Ag_6]^{6+}$	$[Ag_2(\mathbf{5})_2](OTf)_2$	$[Ag_2(\mathbf{5})_2](BF_4)_2$	$[Ag_6(\mathbf{L})_3](OTf)_3(PF_6)_3$
formula	$C_{34}H_{38}F_4N_6$	$C_{84}H_{92}Ag_2F_{20}N_{20}P_2$	$C_{120}H_{132}Ag_6F_{30}N_{24}O_{18}S_6$	$C_{44}H_{68}Ag_2F_6N_{12}O_8S_2$	$C_{43}H_{72}Ag_2B_2F_8N_{12}O_3$	$C_{111}H_{123}Ag_6F_{39}N_{21}O_9P_3S_3$
formula weight	606.70	2039.45	3608.07	1286.96	1194.48	3472.61
Temperature (K)	173(2)	173(2)	173(2)	160(2)	90(2)	173(2)
crystal system	Monoclinic	Triclinic	Trigonal	Orthorhombic	Monoclinic	Trigonal
space group	$P2_1/c$	P-1	$R3$	$Pbca$	$P2_1/c$	$R3$
Z	4	1	3	8	4	3
a (Å)	8.811(5)	12.056(2)	35.3157(13)	24.3004(18)	13.7283(9)	34.798(4)
b (Å)	12.906(6)	12.485(2)	35.3157(13)	16.3177(9)	15.9798(11)	34.798(4)
c (Å)	29.172(14)	15.558(3)	10.7445(8)	27.233(2)	23.4472(15)	10.7303(11)
α (°)	90	88.585(2)	90	90	90	90
β (°)	105.916(16)	80.567(3)	90	90	97.7780(10)	90
γ (°)	90	83.235(3)	120	90	90	120
V (Å^3)	3190(3)	2294.0(7)	11605.2(12)	10798.6(13)	5096.4(6)	11252(3)
D_{calc}(g/cm^3)	1.263	1.476	1.549	1.583	1.557	1.537
μ (mm^{-1})	0.093	0.557	0.926	0.884	0.849	0.945
$2\theta_{max}$ (°)	52	52	52	48	52	52
reflections collected	21251	12762	20378	30315	36884	21960
independent reflections	7285 [R_{int} = 0.0753]	8810 [R_{int} = 0.0500]	8686 [R_{int} = 0.0490]	6974 [R_{int} = 0.0484]	12655 [R_{int} = 0.0189]	7901 [R_{int} = 0.0892]
goodness-of-fit on F^2	0.907	1.080	1.067	1.019	1.066	1.603
R_1, wR_2[I > 2σ(I)]	0.0712, 0.1779	0.0671, 0.1843	0.0526, 0.1433	0.0413, 0.0999	0.0312, 0.0779	0.0631, 0.1515
R_1, wR_2[all data]	0.1211, 0.2099	0.0808, 0.1998	0.0549, 0.1445	0.0593, 0.1115	0.0365, 0.0813	0.0844, 0.1746

Table S2. Selected bond lengths (Å) and bond angles (°) for $[(\mathbf{L})_2Ag_2]^{2+}$

Ag1-N1	2.487(4)	Ag1-N2	2.465(4)
Ag1-N3	2.548(5)	Ag1-N4	2.470(4)
Ag1-N5A	2.250(4)		
N5A-Ag1-N2	122.37(14)	N5A-Ag1-N4	117.80(14)
N2-Ag1-N4	118.11(14)	N5A-Ag1-N1	132.83(14)
N2-Ag1-N1	75.14(17)	N4-Ag1-N1	75.07(18)
N5A-Ag1-N3	109.49(14)	N2-Ag1-N3	73.76(17)
N4-Ag1-N3	74.27(19)	N1-Ag1-N3	117.63(14)

Symmetry code: A) -x+1, -y+1, -z

Table S3. Selected bond lengths (Å) and bond angles (°) for $[(\mathbf{L})_3Ag_6]^{6+}$

Ag1-N1	2.462(7)	Ag1-N2	2.525(7)
Ag1-N3	2.517(7)	Ag1-N4	2.418(7)
Ag1-N7	2.252(8)	Ag2-N5	2.120(8)
Ag2-N6A	2.142(8)		
N7-Ag1-N4	137.4(3)	N7-Ag1-N1	133.3(3)
N4-Ag1-N1	78.0(2)	N7-Ag1-N3	102.0(3)
N4-Ag1-N3	75.4(2)	N1-Ag1-N3	118.9(2)
N7-Ag1-N2	99.5(3)	N4-Ag1-N2	119.3(2)
N1-Ag1-N2	73.8(2)	N3-Ag1-N2	73.4(2)
N5-Ag2-N6A	170.6(4)		

Symmetry code: A) -x+y, -x, z

Table S4. Selected bond lengths (Å) and bond angles (°) for $[Ag_2(\mathbf{5})_2](OTf)_2$

Ag1-N1	2.560(4)	Ag1-N2	2.522(4)
Ag1-N3	2.428(5)	Ag1-N4	2.504(4)
Ag1-N11	2.287(4)	Ag2-N5	2.305(4)
Ag2-N7	2.544(4)	Ag2-N8	2.524(4)
Ag2-N9	2.446(5)	Ag2-N10	2.488(4)
N11-Ag1-N3	117.29(15)	N11-Ag1-N4	100.65(15)
N3-Ag1-N4	73.76(15)	N11-Ag1-N2	142.08(15)
N3-Ag1-N2	75.34(13)	N4-Ag1-N2	117.26(14)
N11-Ag1-N1	121.01(15)	N3-Ag1-N1	116.69(15)
N4-Ag1-N1	73.49(13)	N2-Ag1-N1	74.00(13)
N5-Ag2-N9	118.06(15)	N5-Ag2-N10	98.09(15)
N9-Ag2-N10	73.63(16)	N5-Ag2-N8	144.80(15)
N9-Ag2-N8	75.00(15)	N10-Ag2-N8	117.11(15)
N5-Ag2-N7	118.61(14)	N9-Ag2-N7	117.44(15)
N10-Ag2-N7	74.41(13)	N8-Ag2-N7	74.10(13)

Table S5. Selected bond lengths (Å) and bond angles (°) for $[Ag_2(\mathbf{5})_2](BF_4)_2$

Ag1-N1	2.5848(14)	Ag1-N2	2.4749(15)
Ag1-N3	2.4278(16)	Ag1-N4	2.4990(15)
Ag1-N11	2.2684(15)	Ag2-N5	2.2715(15)
Ag2-N7	2.6177(15)	Ag2-N8	2.4937(15)
Ag2-N9	2.4174(16)	Ag2-N10	2.4875(15)
N11-Ag1-N3	123.05(5)	N11-Ag1-N2	144.51(5)
N3-Ag1-N2	75.77(5)	N11-Ag1-N4	96.50(5)
N3-Ag1-N4	73.95(5)	N2-Ag1-N4	118.51(5)
N11-Ag1-N1	113.04(5)	N3-Ag1-N1	117.15(5)
N2-Ag1-N1	74.60(5)	N4-Ag1-N1	73.87(5)
N5-Ag2-N9	123.90(5)	N5-Ag2-N10	99.97(5)
N9-Ag2-N10	73.78(5)	N5-Ag2-N8	142.20(5)
N9-Ag2-N8	75.77(5)	N10-Ag2-N8	117.28(5)
N5-Ag2-N7	114.03(5)	N9-Ag2-N7	116.71(5)
N10-Ag2-N7	73.37(5)	N8-Ag2-N7	73.73(5)

References

S1. *APEX2 Version 2009.1-0 Data collection and Processing Software*; Bruker AXS Inc.: Madison, Wisconsin, U.S.A., **2008**.

S2. Sheldrick, G. M. Crystal structure refinement with *SHELXL*. *Acta Cryst.* **2015**, *C71*, 3–8.

S3. Spek, A. L. PLATON SQUEEZE: a tool for the calculation of the disordered solvent contribution to the calculated structure factors. *Acta Cryst.* **2015**, *C71*, 9-18.